water

Design and Bench-Scale Hydrodynamic Testing of Thin-Layer Wavy Photobioreactors

Monica Moroni, Simona Lorino, Agnese Cicci and Marco Bravi

The modelling of the photobioreactor with the ANSYS Fluent® software was done both with a mesh of quadrangular cells (19,400 cells) and with an unstructured mesh of triangular cells (27,400 cells). Figure S1 illustrates both arrangements.

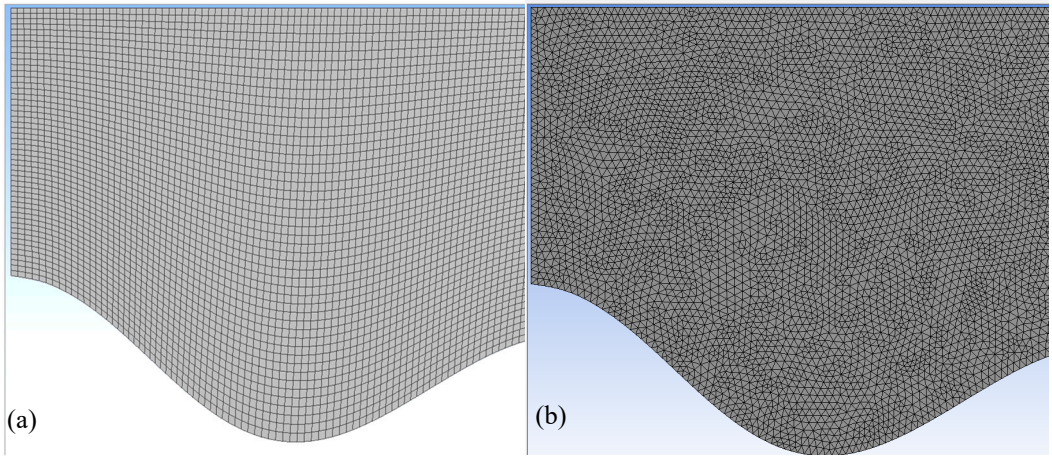


Figure S1. Model domain with (**a**) quadrangular and (**b**) triangular mesh cells.

The simulation led to a two-phase flow, hence the special importance of an accurate tracking of the interface position. Both implicit and explicit resolution schemes for the VOF model were investigated. Figure S2 compares the colour maps of the water volume fraction obtained by employing (a) implicit Volume of Fraction and (b) explicit Volume of Fraction models.

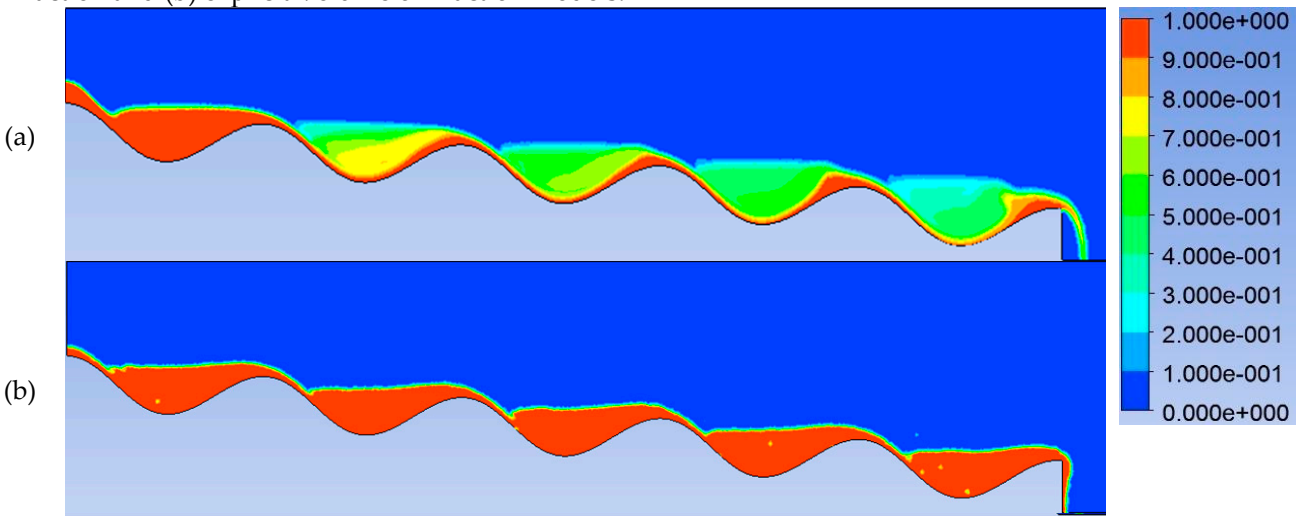


Figure S2. Color maps of the water volume fraction obtained by employing the (**a**) implicit Volume of Fraction and (**b**) explicit Volume of Fraction models (recall that the red color represents water, while blue air).

A further factor that strongly affects the accuracy of interface tracking is the size of the calculation grid. Figure S3 compares the results obtained with quadrangular calculation grids with increasing size (10^{-3} m; 2×10^{-3} m and 3×10^{-3} m).

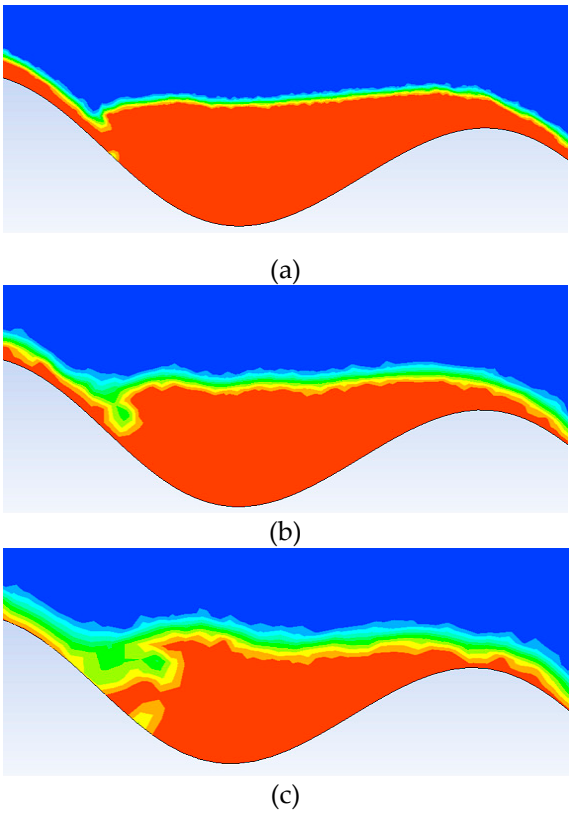
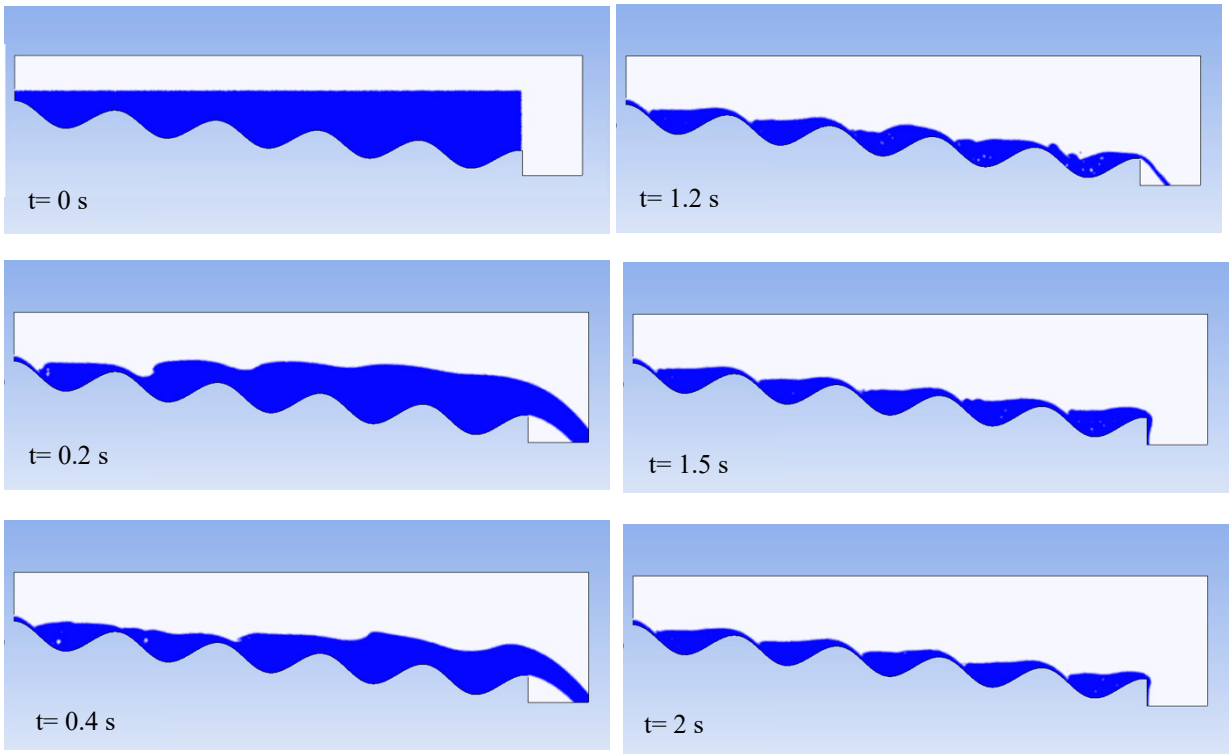


Figure S3. Comparison of the interface for quadrangular cells of (**a**) 10^{-3} m, (**b**) 2×10^{-3} m and (**c**) 3×10^{-3} m size.

Figure S4 shows the time history of the water volume fraction (water is indicated in blue).



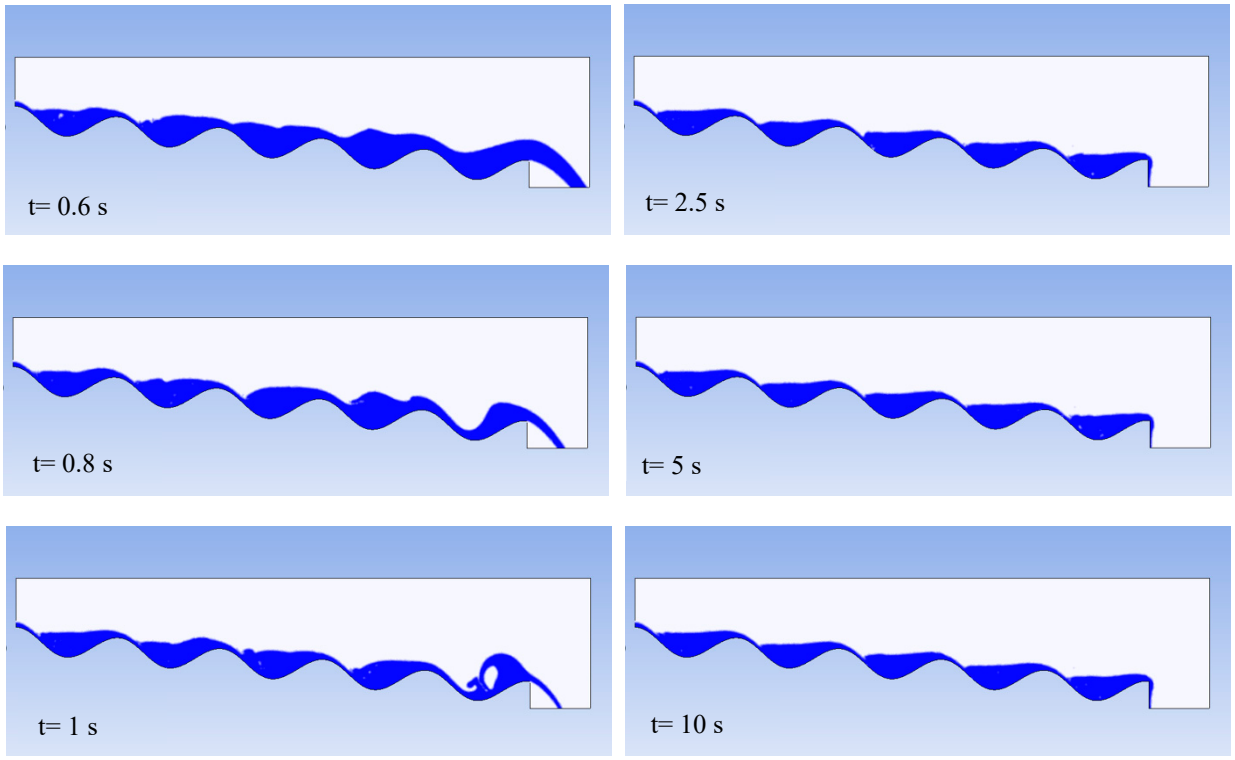


Figure S4. Time history of the water volume fraction.

The kinematic behavior of the photobioreactor is reported by resorting to streamlines (i.e., the family of curves that are instantaneously tangent to the velocity vector of the flow). Figures S5 and S6 display streamlines from numerically and experimentally detected data, respectively, corresponding to the three different flow rates relevant to the channel inclined by 6°. An evident feature of all the streamlines plots is the simultaneous presence of two characteristic flow zones, identified by a different coloring, each referring to a specific stream: the red stream identifies a transport (or straight flow) stream, which is present at any longitudinal abscissa of the photobioreactor and characterizes the part of the liquid which is in contact with the wavy bottom and features a roughly constant thickness. Above the red stream, blue isolated zones can be observed in every cavity, characterizing local recirculation zones, whence the nickname which was attached to the photobioreactor. These local recirculation zones become noticeably smaller as the specific flow rate becomes larger.

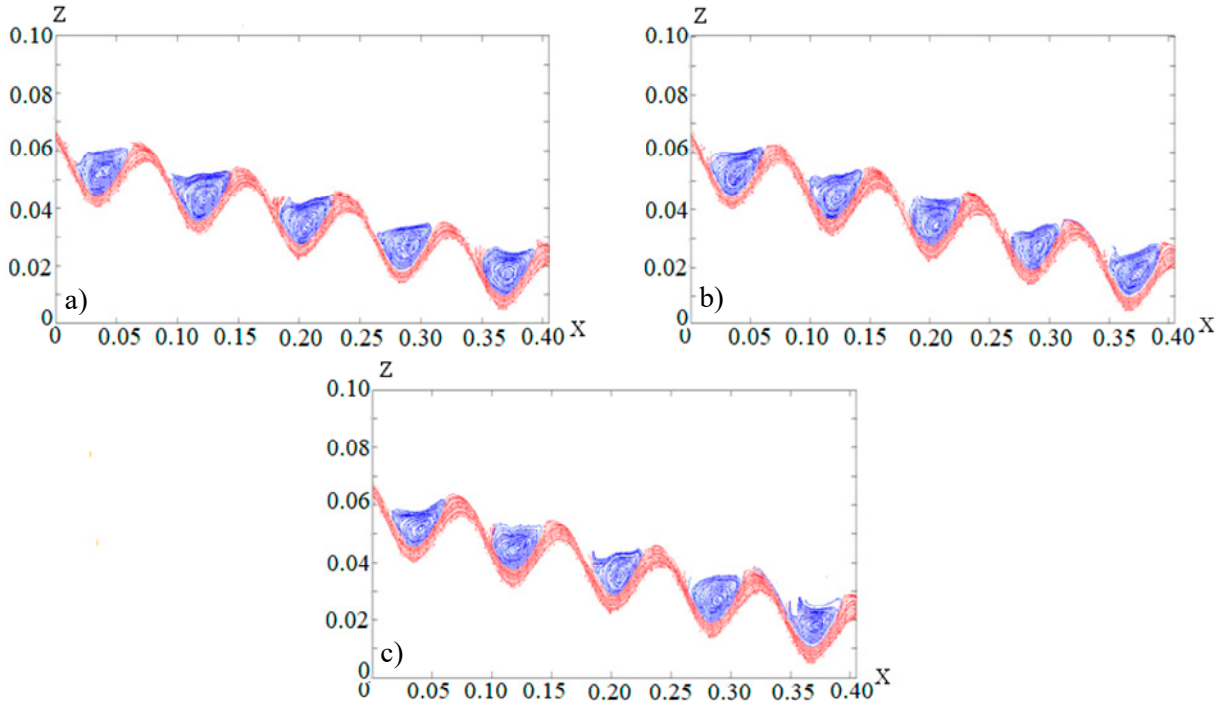


Figure S5. Streamlines from numerical data for 6° slope and flow rate per unit width **a**) 1.11 × 10^{-3} m^3 s^{-1} m^{-1}; **b**) 1.48 × 10^{-3} m^3 s^{-1} m^{-1} and **c**) 1.85 × 10^{-3} m^3 s^{-1} m^{-1} (streamlines refer to the condition reached at simulation time = 4 s with 1 mm quadrilateral calculation grid).

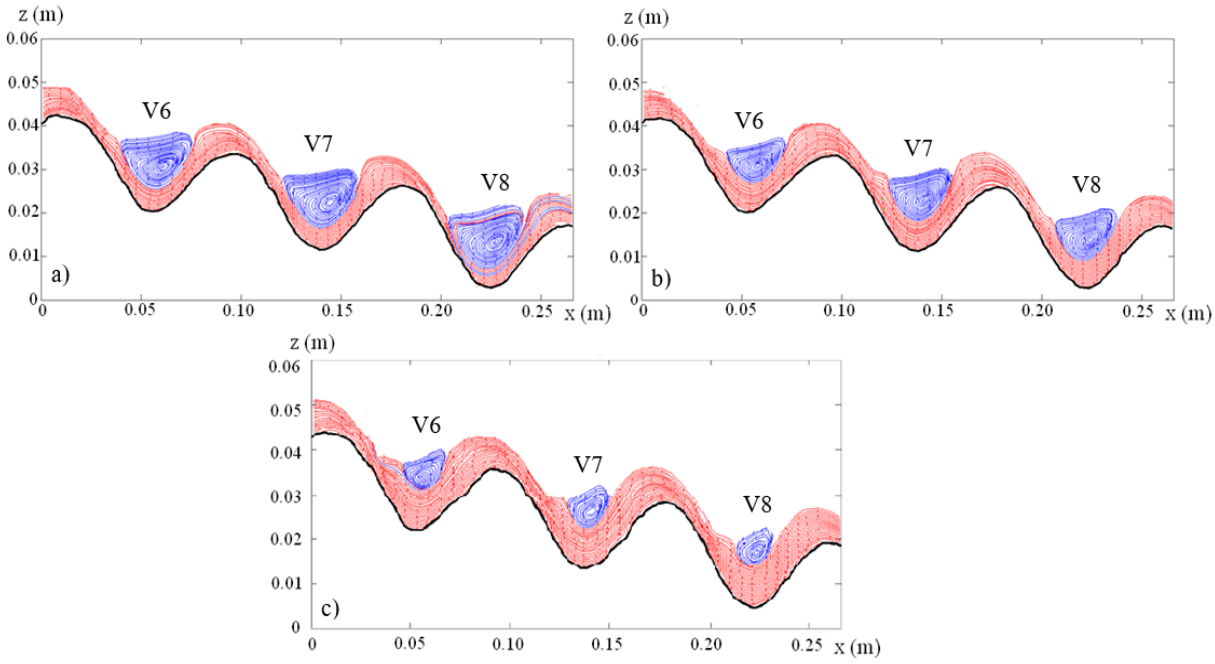


Figure S6. Streamlines from experimental data for 6° slope and flow rate per unit width **a**) 1.11 × 10^{-3} m^3 s^{-1} m^{-1}; **b**) 1.48 × 10^{-3} m^3 s^{-1} m^{-1} and **c**) 1.85 × 10^{-3} m^3 s^{-1} m^{-1}.

The simulations relevant to the channel inclined by 9° are characterized by the presence of a less stable free surface with respect to that obtained in the cases with channel inclination equal to 6° and the recirculation zones, although they are present, do not affect well-defined zones (i.e., they fluctuate over time) even when

the simulation has reached the steady state. As an example, by enlarging a vane relevant to the intermediate specific flow rate multiple vortices can be noticed in the zone above the transport stream (Figure S7).

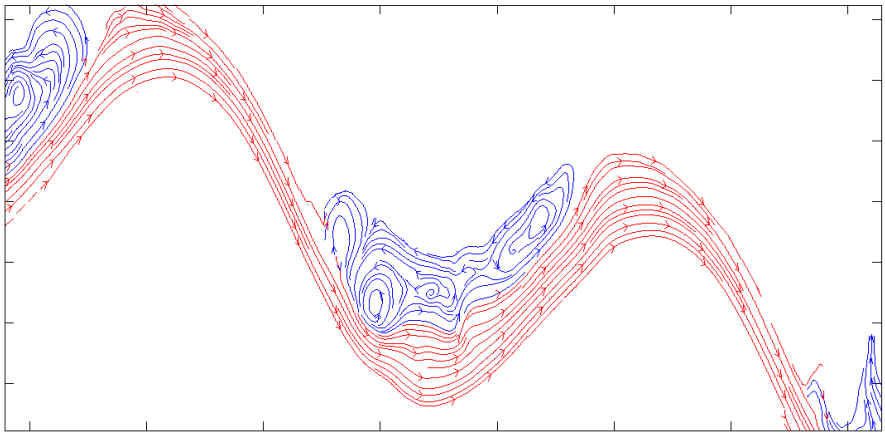


Figure S7. Magnification of a single vane (slope 9°, specific flow rate = 1.48×10^{-3} $m^3 s^{-1} m^{-1}$).